

Critical scales in anisotropic spin systems from functional renormalization

Stefan Göttel,^{1,2} Sabine Andergassen,^{1,2,3} Carsten Honerkamp,^{2,4} Dirk Schuricht,^{1,2} and Stefan Wessel^{2,4,5}

¹*Institute for Theory of Statistical Physics, RWTH Aachen, 52056 Aachen, Germany*

²*JARA-Fundamentals of Future Information Technology*

³*Faculty of Physics, University of Vienna, Boltzmanngasse 5, 1090 Vienna, Austria*

⁴*Institute for Theoretical Solid State Physics, RWTH Aachen, 52056 Aachen, Germany*

⁵*JARA-High-Performance Computing*

(Dated: February 15, 2012)

We apply a recently developed functional renormalization group (fRG) scheme for quantum spin systems to the spin-1/2 antiferromagnetic XXZ model on a two-dimensional square lattice. Based on an auxiliary fermion representation we derive flow equations which allow a resummation of the perturbation series in the spin-spin interactions. Spin susceptibilities are calculated for different values of the anisotropy parameter. The phase transition between planar and axial ordering at the isotropic point is reproduced correctly. The results for the critical scales from the fRG as quantitative measures for the ordering temperatures are in good agreement with the exact solution in the Ising limit. On the easy-plane side, the deviations from critical temperatures obtained with quantum Monte Carlo are larger but still acceptable. However, at the isotropic point the Mermin-Wagner theorem is violated such that a precise description of the behavior in the vicinity of the phase transition is not possible. We discuss possible reasons for these discrepancies.

PACS numbers: 05.10.Cc, 75.10.Jm, 75.30.Kz, 75.50.Ee

I. INTRODUCTION

Renormalization group (RG) methods for fermions developed over the last decades have become a widely used tool for correlated electron systems^{1–4}. Besides a qualitative understanding of fundamental low-energy aspects of weakly interacting many-fermion systems such as the stability of Fermi liquids^{2,5} or the effective behavior of impurities in Luttinger liquids^{6,7}, RG methods have also been used extensively for investigating competing ordering tendencies in two-dimensional lattice systems or the different regimes in impurity problems in one or zero dimensions^{4,8}. Functional RG (fRG) methods do not only concentrate on a smaller number of possibly relevant terms in the theory, but aim to resolve the flow of the generating functional of the theory or the respective vertex functions in as much detail as possible. This allows one to monitor how effects at intermediate energy scales drive the flow to certain fixed points, and at which scales typical low-energy behaviors such as power-laws or scaling should actually hold. While for bosonic problems one can implement the fRG non-perturbatively^{9,10}, for fermionic problems^{4,10} one has to work with a truncation in the powers of fermionic fields. This usually restricts the validity to weak to moderate interaction strengths. Many applications use the fRG method primarily as a qualitative tool for the exploration of theoretical pathways to different low-energy behaviors. Nevertheless, it is important to note that for most cases alluded to above, the approach is controllable in the limit of small interaction strengths. For example, the exponents in Luttinger liquids obtained using the fRG are consistent with non-perturbative or exact solutions⁶. Likewise, the d -wave superconducting pairing instability in the two-dimensional Hubbard model can be seen to be immune against cor-

rections in the limit of small interactions¹¹.

Competing orders and strong quantum fluctuations are also encountered in quantum spin systems^{12,13}. In this very active research area, analytical or field theoretical approaches are however even more involved than for moderately interacting fermions due to the constraint of a fixed total spin per lattice site. Direct numerical methods are often the most reliable approach to these strongly correlated problems, but finite-size effects and sign problems due to frustration effects can make it difficult to obtain clear results. Hence new methods might help. Recently, the fRG has been formulated for auxiliary $S = 1/2$ fermions describing localized quantum spins. In a series of papers^{14–20} it was shown that this approach gives qualitatively appealing results e.g. for frustrated systems on various two-dimensional lattices. As known from other problems, one advantage of the fRG with respect to other numerical methods is the flexibility in treating different lattice geometries and dimensions. With manageable numerical effort one can study rather large, frustrated systems without encountering sign problems. The formulation is transparent; for example, competing trends can be identified and manipulated (by modifying terms) in the calculations. Hence, it is an interesting question how far the spin-fRG approach can be pushed and how it compares quantitatively to other methods, in cases where benchmarking is possible.

Testing the spin-fRG is also interesting from a theoretical point of view, for several reasons. Expressing the localized spins in terms of auxiliary fermions brings some important differences with respect to 'normal' fermions on a lattice. (i) As mentioned above, the auxiliary fermion number on each site should remain constrained to a fixed value in order to guarantee a faithful representation of the localized quantum spins. Most of the pre-

vious applications of the spin-fRG used a mean-field-like approximation at $T = 0$ where the constraint is treated on average. We will adopt this approximation here as well. In Ref. 14 the authors also report on the possibility to go beyond this approximation by using an imaginary chemical potential²¹ at nonzero temperature T . However, this implies a substantial increase in the numerical effort and we do not consider this option here. (ii) The bare action in terms of the auxiliary fermions does not contain a kinetic energy, i.e. the auxiliary fermions are dispersionless. This is, of course, a prerequisite for the particle-number constraint. Fortunately, in the fRG for this system the dispersionless character is preserved and the auxiliary fermion self-energy remains local, which also significantly simplifies the numerical treatment. On the other hand, the absence of a kinetic energy means that, at least at $T \rightarrow 0$, the system is strongly coupled, and a priori there is no reason why a perturbative fermionic fRG setup (or any other theory perturbative in the interactions) should work well. (iii) Quadratic interactions between localized spins translate into quartic auxiliary fermion interactions that are bi-local in the lattice index, i.e. consist of two pairs of fermion fields with the same site index. Again, this structure is preserved under the fRG flow. This is a tremendous simplification with respect to the 'normal' fermionic case where in general also interactions with more than two site indices occur. Concluding this discussion of the auxiliary fermionic description one can say that points (i) and (ii) are at least two major uncertainties in the spin-fRG approach. On the positive side, the simplified structure of both the bare and the flowing theory allows one to capture basically the full frequency dependence of the self-energy and the four-point interaction vertices, and in addition makes it possible to include the self-energy feedback in the flow equations without too much effort. This means that in the spin-fRG, one reaches an advanced approximation level (for extended systems in more than one dimension) that has before only been used for impurity systems in very selected cases^{22,23}. Hence, it is a very interesting question how this combination of positive and negative expectations performs if one tries to compare the results with other techniques.

The goal of the present paper is to provide a quantitative test of the spin-fRG. In order to provide a well-understood testing ground, we study the spin-1/2 antiferromagnetic XXZ-model, which as function of the anisotropy parameter is known to exhibit two different orderings, and where the critical temperatures for these orderings show a nontrivial variation. The critical scales Λ_c for these orderings computed with the spin-fRG are compared with the critical temperatures T_c obtained from quantum Monte Carlo (QMC) calculations. We note that while it is in principle possible to implement the spin-fRG for finite temperatures and hence to directly measure T_c , this would drastically increase the numerical effort. Thus in practice one aims to relate the energy scales Λ_c found more easily at $T = 0$ to the ac-

tual T_c . Our work provides insights to where and to what extent this is possible.

This paper is organized as follows: after introducing the anisotropic Heisenberg model, the auxiliary-fermion representation and the technical implementation of the fRG specific to spin systems is shortly reviewed. We then present the results for the spin susceptibility and the critical scales of the fRG as estimates for the critical temperature and discuss the merits and limitations of the spin-fRG.

II. MODEL

In the following, we consider the spin-1/2 XXZ model with antiferromagnetic nearest-neighbor exchange interaction $J > 0$, defined by the Hamiltonian

$$H = J \sum_{\langle ij \rangle} (S_i^x S_j^x + S_i^y S_j^y + \Delta S_i^z S_j^z). \quad (1)$$

Here, \vec{S}_i denotes the spin-1/2 operators on lattice site i of a two-dimensional square lattice with periodic boundary conditions. Furthermore, Δ is the exchange anisotropy, which we restrict to the antiferromagnetic domain, i.e. $\Delta \geq 0$ throughout this study. For the above model, both the ground state properties as well as the finite temperature phase diagram are well established, cf. e.g. Ref. 24. Here, we mention those features that are relevant for our assessment of the spin-fRG method.

In the easy-axis region, $\Delta > 1$, the ground state is Néel-ordered along the longitudinal (z) direction, while within the easy-plane region for $\Delta < 1$, the ground state exhibits long-range transverse antiferromagnetic ordering within the xy -plane. Within the easy-axis region, long-ranged longitudinal Néel-order emerges already below a finite transition temperature $T_c > 0$. This transition corresponds to the breaking of the discrete Z_2 symmetry of H , and thus belongs to the universality class of the two-dimensional Ising model. In particular, in the large- Δ limit, $\Delta \rightarrow \infty$, the transition temperature scales like $T_c \approx 2.269\Delta/4$, as obtained from the exact solution of the two-dimensional Ising model²⁵ (the factor of 1/4 results from the different normalization of the spin variables usually employed in the classical Ising model as compared to the spin-1/2 operators entering H). The ground state ordering in the easy-plane region, i.e. for $\Delta < 1$, relates to the breaking of the $U(1)$ symmetry of H , such that in two dimensions the transverse long-range order does not persist to nonzero temperatures, consistent with the Mermin-Wagner theorem²⁶. Still, the system exhibits a Berezinskii-Kosterlitz-Thouless (BKT) transition^{27,28} at a critical temperature $T_{\text{BKT}} > 0$ driven by the unbinding of vortex excitations above T_{BKT} out of a low-temperature quasi-long-ranged ordered phase with algebraic decay of the transverse spin correlation function. This phase is furthermore characterized by a finite spin stiffness, which exhibits an universal jump at

T_{BKT} . At $\Delta = 1$, the Hamiltonian H exhibits the full $SU(2)$ symmetry and the antiferromagnetic order is constrained to zero temperatures, such that at this isotropic point the critical temperature vanishes, i.e. $T_c = 0$. The Δ -dependence of both the Ising transition temperature and the BKT transition temperature in the vicinity of $\Delta = 1$ has been analyzed in Ref. 29.

However, in order to assess the quality of the spin-fRG approach to the XXZ model, we require an estimation of the critical temperature T_c for a wider range of different Δ -values. Since the model is not frustrated, we can indeed employ numerically exact, unbiased QMC methods for this purpose. Here, the critical temperatures in both the easy-axis and easy-plane regions have been extracted from QMC simulations using the stochastic series expansion method³⁰ with generalized directed loop updates^{31,32}. In particular, we simulated finite lattices with $N = L^2$ spins and with linear system sizes L ranging up to 32 using periodic boundary conditions. From the finite size data, the critical temperature for the Ising transition was obtained from a finite-size analysis based on the critical Binder ratio³³. Within the easy-axis region, the spin stiffness was calculated from measuring the spin winding number fluctuations³⁴. From the universal stiffness jump at the BKT transition, the transition temperature was then obtained³⁵. The values of the transition temperatures for $|\Delta - 1| < 0.1$ can also be taken from Ref. 29 and for $\Delta = 0$ from Ref. 36. The results of these calculations will be presented below. However, before presenting these data, we provide a short introduction to the spin-fRG method in the following section.

III. AUXILIARY FERMIONS AND SPIN-FRG

Here we briefly describe the spin-fRG scheme introduced by Reuther and Wölfle¹⁴. In order to be able to implement the fermionic fRG scheme^{4,37} for the quantum spin system, one chooses a representation of the spin operators in terms of Abrikosov auxiliary-fermions³⁸. This representation requires two fermionic operators $f_{i\alpha}$, $\alpha = \uparrow, \downarrow$, for each lattice site i ,

$$S_i^\mu = \frac{1}{2} \sum_{\alpha\beta} f_{i\alpha}^\dagger \sigma_{\alpha\beta}^\mu f_{i\beta}, \quad (2)$$

with σ^μ being the Pauli matrices. By construction, the representation satisfies the correct commutation relation of spin operators. The advantage of this representation lies in its quadratic form which allows for the application of Feynman-diagram techniques. However, the introduction of auxiliary fermions implies an enlargement of the Hilbert space, as a single site can now also carry total spin zero, either by being empty or by being doubly occupied. In order to obtain a faithful representation of the quantum spin-1/2-system, these unphysical states have to be projected out. This is formally achieved by

the requirement that the single-occupancy operators

$$Q_i = \sum_{\alpha} f_{i\alpha}^\dagger f_{i\alpha} \quad (3)$$

all possess the eigenvalue 1 on any physical state $|\text{phys}\rangle$ occurring in the thermodynamic averages of the fermionic system, i.e. $Q_i|\text{phys}\rangle = |\text{phys}\rangle$. Thus all unphysical states are discarded.

The single-occupancy constraint immensely complicates the fRG treatment. A convenient approximation is to enforce the constraint only on average by requiring $\langle Q_i \rangle = 1$. With this, of course, local particle number fluctuations are still possible. Due to the particle-hole symmetry in the dispersionless pseudo-fermion system $\langle Q_i \rangle = 1$ is fulfilled for $\mu = 0$. For an exact projection without fluctuations, Popov and Fedotov²¹ proved the mutual cancellation of the unphysical contributions at each lattice site in the thermodynamic averages if an imaginary chemical potential $\mu = -i\pi T/2$ is used. However, as the limit $T \rightarrow 0$ and the suppression of fluctuations at $T = 0$ do not necessarily commute, the two procedures need not to be equivalent at $T = 0$. Following Ref. 14 we here consider the average projection $\langle Q_i \rangle = 1$ and vanishing temperature $T = 0$ for simplicity. More details to this point can be found in Ref. 39.

After transforming the initial spin-system into a fermionic one, the requirements to apply the fermionic fRG are fulfilled (except for the lack of a small expansion parameter, see the discussion below). The idea⁴ is to sum up the contributions to the 1-particle irreducible (1PI) vertex functions from high to low energies. To achieve this, we introduce a cutoff Λ into the bare Green's function which is replaced by

$$G^{0,\Lambda}(i\omega) = \frac{\Theta(|\omega| - \Lambda)}{i\omega}. \quad (4)$$

Inserting $G^{0,\Lambda}$ into the generating functional of the 1PI vertices and performing the derivative with respect to Λ leads to an infinite hierarchy of flow equations. For numerical calculations this hierarchy has to be truncated. It turns out that a truncation after the four-point vertex in the straightforward form of the 1PI fRG hierarchy³⁷ is not sufficient to adequately describe the competition between order and disorder fluctuations¹⁴. An improved scheme suggested by Katanin⁴⁰ includes more self-energy corrections such that Ward identities^{41,42} are better fulfilled. With this Katanin-modification, which we will use as well, the results for the J_1 - J_2 -model were found¹⁴ to be in good agreement with other studies. However, we will see that the spin fRG still overestimates the magnetic ordering tendencies during the flow. Unfortunately, due to the increasing numerical effort the inclusion of higher-order contributions beyond the Katanin truncation scheme is not feasible.

Within the Katanin-modified 1PI-scheme, the RG equations for the self-energy Σ^Λ and the 2-particle vertex

Γ^Λ read

$$\frac{d}{d\Lambda}\Sigma_1^\Lambda = -\frac{1}{2\pi}\sum_2\Gamma_{1,2;1,2}^\Lambda S^\Lambda(\omega_2) \quad (5)$$

$$\begin{aligned} \frac{d}{d\Lambda}\Gamma_{1',2';1,2}^\Lambda = & -\frac{1}{2\pi}\sum_{3,4}\left[\Gamma_{1',2';3,4}^\Lambda\Gamma_{3,4;1,2}^\Lambda\right. \\ & -\Gamma_{1',4;1,3}^\Lambda\Gamma_{3,2';4,2}^\Lambda - (3 \leftrightarrow 4) \\ & \left. +\Gamma_{2',4;1,3}^\Lambda\Gamma_{3,1';4,2}^\Lambda + (3 \leftrightarrow 4)\right] \\ & \times G^\Lambda(\omega_3)\frac{d}{d\Lambda}G^\Lambda(\omega_4) \end{aligned} \quad (6)$$

where the multi-indices $1 = \omega_1, i_1, \alpha_1$ include the frequency, site and spin, and the sum over 1 contains an integral over ω_1 as well as a sum over i_1 and α_1 . Furthermore,

$$G^\Lambda(i\omega) = \frac{\Theta(|\omega| - \Lambda)}{i\omega - \Sigma^\Lambda(i\omega)} \quad (7)$$

is the full propagator and

$$S^\Lambda(i\omega) = \frac{\delta(|\omega| - \Lambda)}{i\omega - \Sigma^\Lambda(i\omega)} \quad (8)$$

denotes the single-scale propagator. The self-energy is a purely imaginary odd function of the frequency and can be written in the form

$$\Sigma_i^\Lambda(i\omega) = -i\gamma^\Lambda(\omega). \quad (9)$$

We observe that in the diagrammatic expansion the Green's function remains strictly local¹⁴ and the momentum dependence of the susceptibility is generated by the non-local exchange couplings. If one uses the symmetry relations of the system and energy conservation, one can parametrize the 2-particle vertex in the form

$$\begin{aligned} \Gamma_{1',2';1,2}^\Lambda = & \left[\Gamma_{zi_1i_2}^\Lambda(s, t, u)\sigma_{\alpha_1'\alpha_1}^z\sigma_{\alpha_2'\alpha_2}^z\right. \\ & +\Gamma_{xyi_1i_2}^\Lambda(s, t, u)(\sigma_{\alpha_1'\alpha_1}^x\sigma_{\alpha_2'\alpha_2}^x + \sigma_{\alpha_1'\alpha_1}^y\sigma_{\alpha_2'\alpha_2}^y) \\ & \left. +\Gamma_{di_1i_2}^\Lambda(s, t, u)\delta_{\alpha_1'\alpha_1}\delta_{\alpha_2'\alpha_2}\right] \times \delta_{i_1'i_1}\delta_{i_2'i_2} \\ & -\left[\Gamma_{zi_1i_2}^\Lambda(s, u, t)\sigma_{\alpha_1'\alpha_2}^z\sigma_{\alpha_2'\alpha_1}^z\right. \\ & +\Gamma_{xyi_1i_2}^\Lambda(s, u, t)(\sigma_{\alpha_1'\alpha_2}^x\sigma_{\alpha_2'\alpha_1}^x + \sigma_{\alpha_1'\alpha_2}^y\sigma_{\alpha_2'\alpha_1}^y) \\ & \left. +\Gamma_{di_1i_2}^\Lambda(s, u, t)\delta_{\alpha_1'\alpha_2}\delta_{\alpha_2'\alpha_1}\right] \times \delta_{i_1'i_2}\delta_{i_2'i_1} \end{aligned} \quad (10)$$

with 'Mandelstam'-variables $s = \omega_1 + \omega_2$, $t = \omega_{1'} - \omega_1$ and $u = \omega_1 - \omega_{2'}$. To be more precise, the vertices depend only on the difference $|i_1 - i_2|$ due to translational invariance. The resulting RG equations for $\gamma(\omega)$, $\Gamma_{zij}(s, t, u)$, $\Gamma_{xyij}(s, t, u)$, and $\Gamma_{dij}(s, t, u)$ including the full frequency dependence are explicitly stated in Ref. 43. The initial conditions are

$$\gamma^{\Lambda=\infty} = 0, \quad (11)$$

$$\Gamma_{xyi_1i_2}^{\Lambda=\infty}(s, t, u) = \begin{cases} \frac{1}{4}J & \text{for } |i_1 - i_2| = 1, \\ 0 & \text{otherwise,} \end{cases} \quad (12)$$

$$\Gamma_{zi_1i_2}^{\Lambda=\infty}(s, t, u) = \begin{cases} \frac{\Delta}{4}J & \text{for } |i_1 - i_2| = 1, \\ 0 & \text{otherwise,} \end{cases} \quad (13)$$

$$\Gamma_{di_1i_2}^{\Lambda=\infty}(s, t, u) = 0. \quad (14)$$

We note that the spatial structure of the interactions only enters the initial conditions.

We can also drop some terms in this 'full' set of fRG equations and thereby reproduce single-channel summations of random-phase-approximation (RPA) character. Below we will present RPA data from such a restricted flow, where only specific terms in the t -channel ($\sim \Gamma_{1',4;1,3}^\Lambda\Gamma_{3,2';4,2}^\Lambda + (3 \leftrightarrow 4)$) of the flow equation (6) for the 2-particle vertex are taken into account, as explained in Ref. 14. Inserting the representation (10) into the t -channel gives various terms. The terms involving $\Gamma_{di_1i_2}^\Lambda$ remain zero, as the initial condition $\Gamma_{di_1i_2}^{\Lambda=\infty} = 0$ is conserved in the flow with the t -channel only. The remaining terms can be analyzed most easily by Fourier-transforming the vertices $\Gamma_{z/xy i_1 i_2}^\Lambda$ from $i_1 - i_2$ to \vec{q} . In reciprocal space, the vertices only depend on one wave-vector \vec{q} . In the t -channel for the flow of $\Gamma_{z/xy \vec{q}}^\Lambda$ there are now terms that do not couple different \vec{q} s, while other terms contain an internal sum over another wave-vector \vec{q}' . The first class of terms can be interpreted as bubble-like RPA, while the second class could be called vertex corrections, and are dropped in the RPA-approximation. This leads to the RPA-like flow equation for the vertex, explicitly written out in Eq. (40) in Ref. 14. We discuss two versions: In the "RPA0" the self-energy is neglected, whereas for the "RPA+" self-energy contributions are taken into account as in the usual self-consistent RPA without cutoffs. For the flow equation of the self-energy no further selection of the diagrams is necessary, here only a Fock-like contribution remains. Note that in specific fermionic models, integrating the RPA + Hartree terms gives results equivalent to mean-field theory^{40,44}, but RPA + Fock (or, equivalently, mean-field+Fock, as the Hartree term vanishes) as in our case does not allow such an equivalence. Furthermore, note that the self-consistent RPA for the 2D Heisenberg-antiferromagnet containing the same class of RPA + Fock diagrams has been found to prevent long-range order at $T > 0$ in accordance with the Mermin-Wagner theorem, but at the price of overdamping the spin-wave excitations at small frequencies⁴⁵. When comparing this to the RPA+, it is important to note that while diagrams with the same topology are used, the propagators on the internal lines differ, and in general the fRG results integrated down to zero scale cannot be expected to match those of self-consistent schemes.

IV. RESULTS

We have solved the RG equations (5) and (6) with the initial conditions (11)–(14) numerically. Following Ref. 14 we used a logarithmic frequency discretization of

$N_f = 30$ positive frequencies, if it is not explicitly stated otherwise, with $\omega_{min} = 0.001J$ and $\omega_{max} \approx 250J$. This ensures that the small frequencies are covered in detail and some frequencies higher than $\Delta \times J$ are used. Negative frequencies are implicitly included via symmetry relations. Unless stated otherwise, all results were obtained for a lattice with 10×10 sites. Different from the original treatment by Reuther and Wölfle¹⁴, the interactions are not truncated in range. Instead periodic boundary conditions are used.

A. Susceptibility

First we compute the static longitudinal spin-spin correlation function χ_{ij}^{zz} by a diagrammatic calculation

$$\chi_{ij}^{zz}(i\nu = 0) = \int_0^\infty d\tau \langle T_\tau [S_i^z(\tau) S_j^z(0)] \rangle \quad (15)$$

[illegible]

and obtain the Néel susceptibility χ^{zz} through

$$\chi^{zz}[\mathbf{q} = (\pi, \pi), \omega = 0] = \sum_j (-1)^{j_x + j_y} \chi_{0j}^{zz}(i\nu = 0) , \quad (16)$$

where j_x (j_y) denotes the distance in x (y)-direction to an arbitrarily chosen reference point. The transverse spin-spin correlation function χ_{ij}^{xx} is defined analogously. These quantities only have a strict physical interpretation at $\Lambda = 0$, but we will consider them for finite Λ as well and interpret a divergent flow as an indicator for a magnetic instability of the system. Again, using the physical temperature as a cutoff or working at $T > 0$ would make this interpretation more straightforward, but would also strongly increase the numerical effort. The experience from other fermionic systems⁴⁶ shows that divergences with respect to Λ and T are qualitatively equivalent.

The results for different anisotropies Δ are shown in Fig. 1. For $\Delta < 1$ we find a dominating transverse susceptibility χ^{xx} , whereas for $\Delta > 1$ the longitudinal susceptibility χ^{zz} diverges at a larger scale Λ . At the isotropic point $\Delta = 1$ both susceptibilities are identical as required by the full $SU(2)$ invariance. This finding thus reproduces the well-known²⁴ phase transition between planar and axial ordering at $\Delta = 1$. Furthermore, it has to be stressed that due to the generic divergence of the RG flow at a finite scale Λ_c it is impossible to obtain quantitative results for the susceptibility which could be compared to other methods on an absolute scale.

B. Critical scales and temperatures

In Ref. 19 Reuther *et al.* directly interpret the scale Λ_c , at which the fRG flow diverges, as a critical temperature T_c for the phase transition into the ordered phase. In

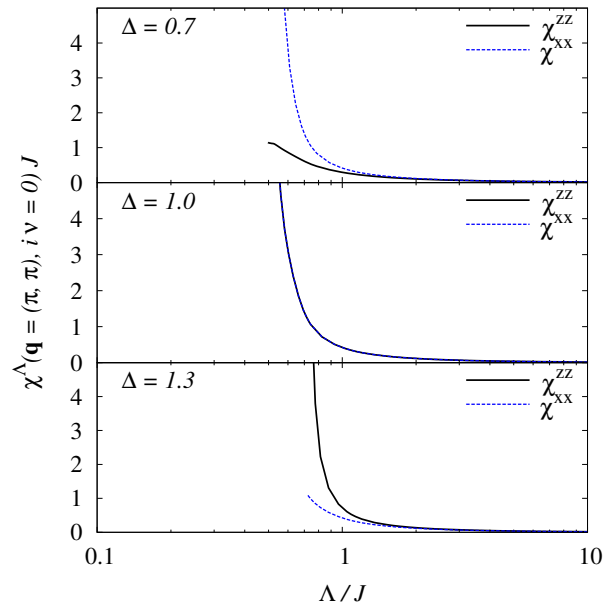


FIG. 1. (Color online) Flow of the static transverse (χ^{xx}) and longitudinal (χ^{zz}) susceptibility for different anisotropy parameters Δ . The results confirm the existence of a phase transition between planar and axial ordering at $\Delta = 1$.

order to test this interpretation we have first studied the dependence of Λ_c on the system size and the frequency discretization. The results shown in Fig. 2 suggest that the scale Λ_c is indeed rather constant at least in the range of lattice sizes studied here. A mild finite-size effect is however visible and indicates that Λ_c tends to increase with system size. As one can see in Fig. 3, for a large enough number of frequencies N_f the scale Λ_c is essentially independent of the discretization. In contrast to the system size dependence no monotonous dependence on N_f is observed. Still for larger Δ , the relative difference in Λ_c for different numbers of frequencies becomes smaller.

As a next test we analyze the Ising limit ($\Delta \rightarrow \infty$) for which the scale Λ_c is shown in Fig. 4. As discussed in Sec. II, the critical temperature $T_c = 2.269\Delta/4$ is known exactly in this limit. We observe that as a function of large Δ the values of Λ_c of the RPA0, the RPA+ and the spin-fRG converge, but that the limiting values differ. Comparing the result for the RPA0 and RPA+ approximations we conclude that the inclusion of the self-energy improves the results, but that both methods still overestimate the ordering tendencies of the system. The spin-fRG presents an improvement over the RPA as the calculated Λ_c agrees rather well with the critical temperature T_c in the Ising limit. From this finding we may conclude that Λ_c can indeed be interpreted as a critical temperature $\Lambda_c = T_c$ (at least in the Ising limit). However, as we show next, this interpretation becomes less satisfactory when leaving the regime of strong Ising anisotropy.

In particular, we consider the regime $\Delta \approx 1$ where

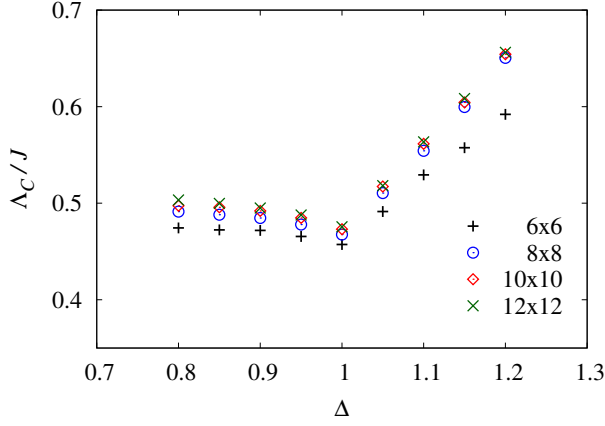


FIG. 2. (Color online) Critical flow parameter Λ_c extracted from the divergence of the spin-fRG flow as a function of the anisotropy parameter Δ for different system sizes. Λ_c increases with the system size.

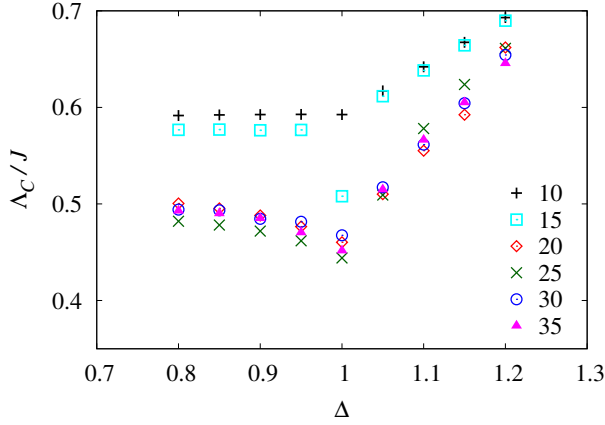


FIG. 3. (Color online) Critical scale Λ_c for different numbers of positive frequencies N_f used in the discretization.

we compare our results with the critical temperature determined from the QMC analysis. As one can see in Fig. 5, the spin-fRG improves the RPA in this regime as well, but the deviation from the QMC results is clearly larger than in the Ising limit. Nevertheless, except for the direct vicinity of the phase transition at $\Delta = 1$, the spin-fRG scale Λ_c correctly describes the dependence of T_c on the anisotropy, and for $\Delta \gtrsim 1.5$ the fRG critical scales Λ_c provides a reasonable quantitative estimate for T_c , whereas for $\Delta \lesssim 0.5$ the difference between fRG and QMC is significant.

The strongest deviations between the critical scale extracted from the spin-fRG and the QMC result are found close to the isotropic point $\Delta = 1$, where the fRG yields a finite critical temperature in violation of the Mermin-Wagner theorem²⁶. Nonetheless the Δ -dependence of T_c obtained in the spin-fRG shows a kink-like feature at $\Delta = 1$, which is not observable in the RPA0 calculation and is only very weak in the RPA+. One may ar-

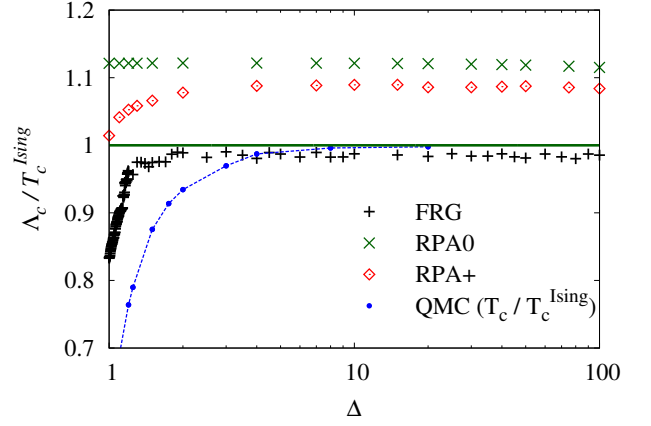


FIG. 4. (Color online) Critical flow parameter Λ_c as obtained from different approaches in comparison to the exact result for the critical temperature in the Ising limit. In comparison to the RPA approaches the spin-fRG reproduces the Ising limit far more correctly. The errors of the QMC data are smaller than the size of the symbols.

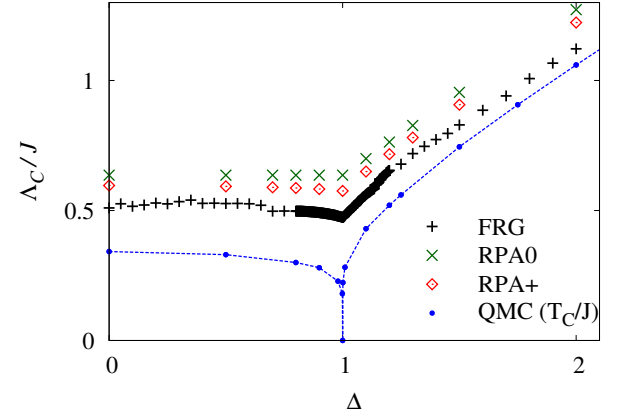


FIG. 5. (Color online) Critical flow parameter Λ_c as a function of the anisotropy parameter Δ near the isotropic point. The errors of the QMC data are smaller than the size of the symbols.

gue that at $T = 0$ ordering indeed occurs and hence the nonzero critical scale obtained from spin-fRG does not violate the Mermin-Wagner theorem. We note, however, that the isotropic Heisenberg model is gapless and it is not clear which energy scale Λ_c thus represents. A more plausible way to understand the data is that the truncated spin-fRG fails to capture a significant part of the physics of collective fluctuations that would be needed to restore $T_c = 0$.

C. Auxiliary fermion self-energy

Closer inspection of the RPA data for Λ_c reveals that RPA+ shows a (weak) kink at $\Delta = 1$ while the RPA0

data are monotonically increasing. The main difference between the two methods is the generated self-energy of the auxiliary fermions. Thus a more detailed analysis of this quantity in the spin-fRG may lead to some insights.

The auxiliary fermion self-energy generated in the spin-fRG is not a physical quantity, since the auxiliary fermion Green's function connects physical and unphysical sectors of the fermionic Hilbert space. Nevertheless, analyzing the self-energy sheds some light on the shortcomings of the spin-fRG and the differences to other methods. At the end of the flow, near Λ_c , the frequency-dependent self-energy $\gamma^\Lambda(\omega)$ shows a peak structure (see Fig. 6), where the maximum occurs at $\omega \approx \Delta$ at least for $\Delta \geq 1$. In this regard, the fRG self-energy qualitatively differs from the one found in self-consistent RPA⁴⁵, which has a peak near zero frequency. The delayed generation of the self-energy in the fRG may be the reason why the self-consistent RPA of Ref. 45 and the RPA+ implemented here do not agree although the same class of diagrams is kept in both approaches.

For a two-site system the exact auxiliary fermion self-energy can be calculated³⁹ at vanishing chemical potential from a Lehmann representation yielding $\gamma \sim 1/\omega$. However, for this case the self-energy generated by the fRG possesses the same form as for the 2D model considered here (see Refs. 43 and 47), i.e. with a peak at nonzero frequency whose position depends on Λ . This difference possibly originates from an incorrect description at small frequencies. Based on this hypothesis, we can give an argument why the spin-fRG critical scales agree with the QMC results for T_c in the Ising limit. Here, the flow diverges already at larger scales Λ . As the self-energy enters the flow equations via the propagators $\sim 1/[\omega + \gamma(\omega)]$, its form for $\omega \geq \Lambda$ only weakly affects the flow. However, for $\Delta \approx 1$, the flow reaches smaller scales and this influence becomes more and more important. This qualitatively explains the good agreement in the Ising limit and may to some extent (more discussion is given further below) account for the failure of the method to correctly describe the critical temperature near the isotropic point and, in particular, the violation of the Mermin-Wagner theorem. Here a stronger (or singular) self-energy at small frequencies would help to avoid the divergence of the flow at a non-zero scale. We note that in self-consistent studies in the auxiliary fermion language⁴⁵ the results could be improved by an artificially introduced stronger suppression of the auxiliary fermion spectral function at small frequencies. Similarly in the spin-fRG, a manipulation towards a larger self-energy at small frequencies would lead to a critical temperature $T_c = 0$ at the Heisenberg point and therefore the fulfillment of the Mermin-Wagner theorem, but the critical temperature especially in the easy-plane regime would be strongly affected and vanishing, too.

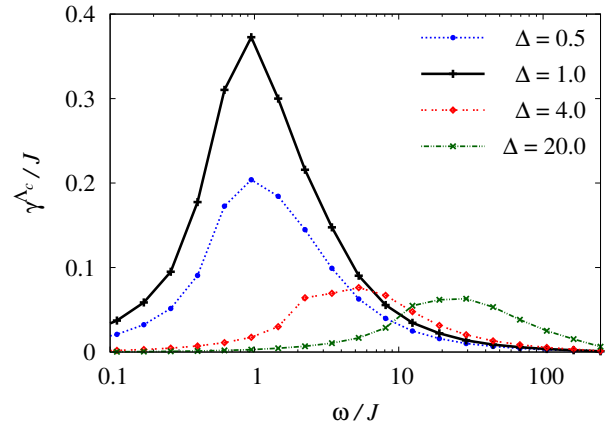


FIG. 6. (Color online) Generated self-energy at the end of the fRG flow, i.e. at $\Lambda = \Lambda_c$, for different values of Δ . During the flow the peak builds up and moves in from higher frequencies.

V. DISCUSSION

The goal of this paper was a comparison of spin-fRG results with those of other methods to perform a qualitative and quantitative assessment of the spin-fRG. We were able to confirm the phase transition between planar and axial ordering at the isotropic point $\Delta = 1$. The identification of the cutoff scale Λ_c with the critical temperature T_c yields rather accurate results in the Ising limit, but at the same time leads to a violation of the Mermin-Wagner theorem at the isotropic Heisenberg point and to deviations in the easy-axis and, to larger degree, in the easy-plane regime. The generated auxiliary fermion self-energy seems too weak to prevent divergences in the fRG flow for $\Lambda_c > 0$. Possible reasons for this error are:

(i) The long-wave physics is not included as the system is still finite. We cannot exclude that the spin waves are just too constrained by our limited system size. We note, however, that for the available system sizes we observe an increasing rather than decreasing Λ_c with system size (see Fig. 2).

(ii) The mapping from the spin- to a fermionic system, where the constraint is fulfilled only on average and does not apply to quantum fluctuations. Here it appears problematic that the auxiliary fermion self-energy remains finite at small frequencies, in contrast with the exact solution of the two-site problem, and possibly in contrast with the requirement of zero particle-number fluctuations of the auxiliary fermions. The finiteness of the self-energy is a consequence of the structure of the frequency flow, and major changes to the formalism may be needed to alter this behavior. This projection problem could also be investigated more systematically by including a nonzero temperature, where an exact projection scheme using an additional imaginary chemical potential is available²¹. The major disadvantage consists in the fact that the imaginary chemical potential breaks vari-

ous symmetries increasing the numerical effort substantially. For the Heisenberg model such calculations have been performed in Ref. 39. As the results showed no qualitative differences to the average projection scheme, it seems that this is not the main source of error.

(iii) The RG treatment of the system with a truncation after the four-point vertex is not controlled because there is no small expansion parameter in the XXZ model. In bosonic descriptions of O(3)-models, the four-boson coupling is essential to drive the critical temperature to zero and hence to fulfill the Mermin-Wagner theorem. In fermionic language, this coupling would correspond to a 1PI eight-fermion vertex that is not present in the truncation used here for the spin-fRG. In this sense, the interaction between low-lying spin fluctuations that suppresses also the zero-frequency ordering might not be implemented correctly in this approach. This is also supported by the observation that the critical scales deviate more strongly from the QMC results for T_c on the easy-plane side where the spin waves are gapless.

Further tests have been performed for one-dimensional models^{43,47}. Here again the spin-fRG performs better than the RPA. For example in the latter there still exists a finite scale Λ_c at which the flow breaks down, while in the former the RG flow can be performed down to the smallest frequency ω_{min} . The spin-fRG correctly reproduces qualitative features like antiferromagnetic correlations. However, on a more quantitative level, the power-law decay of the spatial correlations in the Heisenberg chain is not reproduced by the spin-fRG, which rather predicts an incorrect exponential behavior. Similar shortcomings are seen in other models, e.g. the spin-fRG generically yields too short-ranged correlations in both gapless and for gapped systems. Furthermore the ground-state energies and their dependence on the system parameters and number of lattice sites are not reproduced. Hence, the spin-fRG cannot be regarded as a reliable theoretical method for the study of one-dimensional spin system.

VI. CONCLUSION

In conclusion, the spin-fRG considerably improves RPA results for low-dimensional quantum spin systems. The qualitative behavior of the spin correlations on short scales is reproduced correctly. For the two-dimensional XXZ model studied here, the spin-fRG does detect the quantum phase transition at $\Delta = 1$ and the critical scale Λ_c can be used as an estimate for ordering temperatures away from the isotropic point. For all anisotropies $|\Delta - 1| \gtrsim 0.1$, the deviations in Λ_c from T_c are less than a factor of 2. At the isotropic point $\Delta = 1$, however, the spin-fRG predicts a finite ordering temperature in violation of the Mermin-Wagner theorem, which also spoils the quantitative validity of the spin-fRG results in the vicinity of $\Delta = 1$. Furthermore, as discussed above, due to the generic divergence of the RG flow at a finite scale Λ_c it is impossible to obtain quantitative results for the susceptibilities or correlation functions which could be compared to other methods on an absolute scale. These two drawbacks are well known from the fRG treatment of itinerant two-dimensional many-fermion systems⁴, and also the appealingly advanced approximation level of the spin-fRG with the full-self-energy feedback and frequency-dependence cannot remedy this deficiency. Hence, one may conclude that the spin-fRG should be rather used to explore phase diagrams in situations where strongly differing types of ground states are expected to compete, i.e. ground states that differ in their correlations already on short distances. Such situations were actually addressed in most of the spin-fRG papers up to now.

ACKNOWLEDGMENTS

We thank Johannes Reuther for the helpful exchange on several technical questions, and Wolfram Brenig, Lars Fritz, Andrej Gendiar, Volker Meden, Walter Metzner, Herbert Schoeller, and Ronny Thomale for useful discussions. We particularly thank also Kimmo Sääskilähti for collaboration on the application of the spin-fRG to spin chains. This work was supported by the German Research Foundation (DFG) through FOR 723, FOR 912, and the Emmy-Noether Program (D.S.).

¹ J. Solyom, Adv. Phys. **28**, 201 (1979).

² R. Shankar, Rev. Mod. Phys. **66**, 129 (1994).

³ W. Metzner, C. Castellani, and C. Di Castro, Adv. Phys. **47**, 317 (1998).

⁴ W. Metzner, M. Salmhofer, C. Honerkamp, V. Meden, and K. Schönhammer, accepted by Rev. Mod. Phys; arXiv:1105.5289 (2011).

⁵ M. Salmhofer, *Renormalization: An Introduction* (Springer, Heidelberg, 1999).

⁶ S. Andergassen, T. Enss, V. Meden, W. Metzner, U. Schollwöck, and K. Schönhammer, Phys. Rev. B **70**, 075102 (2004).

⁷ S. Andergassen, T. Enss, V. Meden, W. Metzner, U. Schollwöck, and K. Schönhammer, Phys. Rev. B **73**, 045125 (2006).

⁸ S. Andergassen, T. Enss, C. Karrasch, and V. Meden, in *Quantum Magnetism* edited by B. Barbara, Y. Imry, G. Sawatzky, and P.C.E. Stamp (Springer, New York, 2008).

- ⁹ J. Berges, N. Tetradis, and C. Wetterich, Phys. Rep. **363**, 223 (2002).
- ¹⁰ P. Kopietz, L. Bartosch, and F. Schütz, *Introduction to the Functional Renormalization Group*, Springer Lecture Notes in Physics 798 (Springer, Berlin, 2010).
- ¹¹ The boundedness of corrections to the Cooper channel for generic Fermi surfaces and sufficiently small interactions is, e.g., laid out in the book by M. Salmhofer⁵, but a stringent case study in the fRG framework for the Hubbard model beyond numerical results has not been presented. An in essence equivalent formulation was worked out independently by S. Raghu, S.A. Kivelson and D.J. Scalapino, Phys. Rev. B **81**, 224505 (2010).
- ¹² G. Misguich and C. Lhuillier, in *Frustrated Spin Systems*, edited by H. T. Diep (World Scientific, Singapore, 2005) p. 229.
- ¹³ L. Balents, Nature **464**, 199 (2010).
- ¹⁴ J. Reuther and P. Wölfle, Phys. Rev. B **81**, 144410 (2010).
- ¹⁵ H. Schmidt and P. Wölfle, Ann. Phys. (Berlin) **19**, 60 (2010).
- ¹⁶ J. Reuther and R. Thomale, Phys. Rev. B **83**, 024402 (2011).
- ¹⁷ J. Reuther, P. Wölfle, R. Darradi, W. Brenig, M. Arlego, and J. Richter, Phys. Rev. B **83**, 064416 (2011).
- ¹⁸ J. Reuther, D.A. Abanin, and R. Thomale, Phys. Rev. B **84**, 014417 (2011).
- ¹⁹ J. Reuther, R. Thomale, and S. Trebst, Phys. Rev. B **84**, 100406(R) (2011).
- ²⁰ Y. Singh, S. Manni, J. Reuther, T. Berlijn, R. Thomale, W. Ku, S. Trebst, and P. Gegenwart, arXiv:1106.0429v2 (2012).
- ²¹ V. N. Popov and S. A. Fedotov, Sov. Phys. JETP **67**, 535 (1988).
- ²² C. Karrasch, R. Hedden, R. Peters, Th. Pruschke, K. Schönhammer, and V. Meden, J. Phys.: Condensed Matter **20**, 345205 (2008).
- ²³ S. G. Jakobs, M. Pletyukhov, and H. Schoeller, Phys. Rev. B **81**, 195109 (2010).
- ²⁴ D. J. J. Farnell and R.F. Bishop, in *Quantum Magnetism*, edited by U. Schollwöck, J. Richter, D.J.J. Farnell, and R.F. Bishop, Lecture Notes in Physics Vol. 645 (Springer, Berlin, 2004), p. 323f.
- ²⁵ L. Onsager, Phys. Rev. **67**, 117 (1944).
- ²⁶ N. D. Mermin and H. Wagner, Phys. Rev. Lett. **17**, 1133 (1966).
- ²⁷ V. L. Berezinskii, Sov. Phys. JETP, **32**, 493 (1971).
- ²⁸ J. M. Kosterlitz and D. J. Thouless, J. Phys. C **6**, 1181 (1973).
- ²⁹ A. Cuccoli, T. Roscilde, V. Tognetti, R. Vaia, and P. Ver-rucchi, Phys. Rev. B **67**, 104414 (2003).
- ³⁰ A. W. Sandvik, Phys. Rev. B **59**, R14157 (1999).
- ³¹ O. F. Syljuåsen and A. W. Sandvik, Phys. Rev. E **66**, 046701 (2002).
- ³² F. Alet, S. Wessel, and M. Troyer, Phys. Rev. E **71**, 036706 (2005).
- ³³ K. Binder, Z. Phys. B **43**, 119 (1981).
- ³⁴ E. L. Pollock and D M. Ceperley, Phys. Rev. B **36**, 8343 (1987).
- ³⁵ H. Weber and P. Minnhagen, Phys. Rev. B **37**, 5986 (1988).
- ³⁶ K. Harada and N. Kawashima, Phys. Rev. B **55**, R11949 (1997).
- ³⁷ M. Salmhofer and C. Honerkamp, Prog. Theor. Phys. **105**, 1 (2001).
- ³⁸ A. A. Abrikosov, Physics **2**, 5 (1965).
- ³⁹ J. Reuther, PhD thesis, Universität Karlsruhe (2011).
- ⁴⁰ A. A. Katanin, Phys. Rev. B **70**, 115109 (2004).
- ⁴¹ J. C. Ward, Phys. Rev. **78**, 182 (1950).
- ⁴² T. Enss, PhD thesis, Universität Stuttgart (2005).
- ⁴³ S. Göttel, Master thesis, RWTH Aachen University (2011).
- ⁴⁴ M. Salmhofer, C. Honerkamp, W. Metzner, and O. Lauscher, Prog. Theor. Phys. **112**, 943 (2004).
- ⁴⁵ J. Brinckmann and P. Wölfle, Physica B **359**, 798 (2005).
- ⁴⁶ E.g., in the reduced BCS model for superconductivity with bandwidth W and dimensionless coupling constant $-g$, the fRG in the particle-particle channel gives $\Lambda_c = We^{-1/g}$ and $T_c = 1.14\Lambda_c$.
- ⁴⁷ K. Säskilahti, Master thesis, RWTH Aachen University (2011).